

# GALAXY FORMATION — A CONDENSATION PROCESS JUST AFTER RECOMBINATION

G. LESSNER

FB Physik, Universitt Paderborn, 33098 Paderborn  
Germany

## Abstract

A scenario of galaxy formation is put forward which is a process of sudden condensation just after recombination. It is essentially based on the fact that the cosmic matter gas after recombination is a general relativistic Boltzmann gas which runs within a few  $10^6$  years into a state very close to collision-dominated equilibrium. The mass spectrum of axially symmetric condensation "drops" extends from the lower limit  $M \simeq 10^5 M_\odot$  to the upper limit  $M \simeq 10^{12} M_\odot$ . The lower limit masses are spheres whereas the upper limit masses are extremely thin pancakes. These pancakes contract within a time of about  $2,5 \cdot 10^9 y$  to fastly rotating spiral galaxies with ordinary proportions. In this final state they have a redshift  $z \simeq 3$ . At an earlier time during their contraction they are highly active and are observed with a redshift  $z \simeq 5$ .

PACS numbers: 98.62.Ai; 04.20. - q

## 1. Introduction

The formation of galaxies and large-scale structures in the universe is one of the unsolved problems in the standard model given by the Friedmann–Robertson–Walker–models. Although these models are altogether very successful and therefore widely accepted no way has been found hitherto to explain in this framework the formation of the observed structures in a satisfactory manner.

The essential reason for this lack is the extreme smoothness of the young universe. This smoothness has been verified by the COBE data of the cosmic background radiation. Of course, COBE observed anisotropies  $\Delta T/T \simeq 10^{-5}$  of the background radiation only on a rather large scale of  $7^0$  to  $10^0$ . Hence one might observe on a much smaller scale much larger anisotropies. Nevertheless this would be rather surprising. So it seems that one has to resign to a very smooth universe when it was young. Carrying over the anisotropy  $\Delta T/T \simeq 10^{-5}$  of the background radiation to the density contrast  $\delta \varrho/\varrho \simeq 10^{-5}$  at the end of the recombination period one is confronted with the problem that these contrasts can not grow up to galaxies by gravitational instability in a sufficiently small time [1]. Indeed, today galaxies are observed with redshifts  $z \simeq 5$  which corresponds to about  $10^9 y$  after the big bang. A further problem almost never mentioned is the fact that the galaxies with upper limit masses ( $M \simeq 10^{12} M_\odot$ ) are mainly flat and fastly rotating discs whereas the objects at the lower limit ( $M \simeq 10^5 M_\odot$ ) are spheres.

Today it seems to be proved that the overwhelming part of matter in the universe is non luminous dark matter. This is confirmed by the flat rotation curves in galaxies as well as by gravitational lensing of galaxy clusters. Many cosmologists believe that this dark matter is non baryonic exotic cold dark matter which is subject only to gravitational interaction. They propose a scenario of structure formation which is first of all structure formation in the cold dark matter, the luminous baryonic matter then adds to these structures. The extremely cumbersome numerical calculations yield interesting structures which look very much like to those observed in the universe [2]. However, there are at least two problems in this scenario. First of all, which particles form the cold dark matter? Hitherto there is no experimental evidence for such exotic particles. Secondly, the scenario might perhaps explain the very large-scale structures, it seems, however, not to explain the origin of the single objects — namely the galaxies and the smaller objects down to the globular clusters.

In the following paper we propose a scenario of galaxy formation in an universe without cold dark matter, that means, the dark matter is purely baryonic. A first version of this scenario has been published by the author in two previous paper [3,4]. This version describes only the final state of galaxy formation, not, however, the process. This process has now been understood, and thus the complete scenario can be represented.

The basic idea of the scenario is the fact that the cosmic matter gas is from the end of the recombination period a general relativistic Boltzmann gas which runs within a few  $10^6$  years into a state very close to collision-dominated equilibrium. Hence we sum up briefly from the previous papers [3,4] in sections 2 and 3 the properties of the cosmic matter gas after the recombination period and the properties of a general relativistic Boltzmann gas in collision-dominated equilibrium. In section 4 we describe the process of galaxy formation which is a process of sudden condensation. In section 5 we investigate the time evolution of the condensation ”’drops”’. Finally we discuss our results in a conclusion.

## 2. The cosmic matter gas after recombination

When the universe has cooled down to  $T \simeq 5 \cdot 10^3 K$  the recombination of the cosmic plasma to neutral H- and He-atoms begins. It ends at

$$T \simeq 3 \cdot 10^3 K = T_{rek} \quad (1)$$

when all matter consists of neutral atoms. This recombination period is throughout a drastic event in the history of the universe. One of the important consequences is the drastic change of the range of interaction between the particles. It decreases from the long range Coulomb interaction between charged particles before recombination to the very short range collision interaction between neutral atoms after recombination. In an earlier paper [5] the author argued that the range  $r_c$  of collision interaction in the cosmic matter consisting of 70 % hydrogen and 30 % helium is approximately given by

$$r_c \simeq 7a_0 \quad (2)$$

with Bohr's radius  $a_0$ . Hence we have after recombination the relation

$$r_c n^{1/3} \lesssim 3 \cdot 10^{-7} \quad (3a)$$

with the particle density

$$n = n_H + n_{He} = 0,8 \frac{\rho}{m_p} \quad (3b)$$

( $\rho$  = mass density,  $m_p$  = proton mass). From (3a) we can conclude that the cosmic matter after recombination is a Boltzmann gas. Furthermore the author calculated in [5] the ratio  $t_c/t_{exp}$  where  $t_c$  is the mean time between two collisions and  $t_{exp}$  is the characteristic expansion time of the universe. This ratio takes the value

$$\frac{t_c}{t_{exp}} \simeq 4 \cdot 10^{-8} \left( \frac{T_{rek}}{T} \right)^2, T \leq T_{rek} \quad (4)$$

From this ratio we conclude that the cosmic matter runs from the end of recombination ( $T = T_{rek}$ ) into a state which is very close to equilibrium. But how does this process run and how much time takes it? To answer this question we consider in the following section first of all the final state of this process, namely the general relativistic Boltzmann gas in collision-dominated equilibrium.

### 3. The general relativistic Boltzmann gas in collision-dominated equilibrium

We note that the cosmic matter after recombination runs into a state very close to equilibrium which is not exact the equilibrium. Clearly, the expansion of the universe does not admit an exact equilibrium but only a state very close to equilibrium. Later on we shall assume that the physics of this state is essentially that of exact equilibrium. Thus we deal in this section with a general relativistic Boltzmann gas in collision-dominated equilibrium. For simplicity we assume a one-component gas with particle mass  $m$ .

We adopt the essential properties of a general relativistic Boltzmann gas in collision-dominated equilibrium from the comprehensive reviews given by Stewart [6] and Israel [7]. A space-time filled by such a gas has a time-like killing field

$$\beta^i = \frac{u^i}{kT} \quad (5)$$

where the  $u^i$  are the components of the 4-velocity and  $k$  is Boltzmann's constant (latin indices running from 1 to 4, signature +++-). A reference frame  $\mathcal{K}_0$  can be found such that

$$\beta^i = (0, 0, 0, const) \quad (6)$$

In  $\mathcal{K}_0$  the matter is in rest and the following relations hold

$$g_{ik} = g_{ik}(x^1, x^2, x^3), \quad T = T(x^1, x^2, x^3) \quad (7)$$

$$g_{44}T^2 = const \quad (8)$$

$$mn(x^1, x^2, x^3) = \varrho(x^1, x^2, x^3) = const \cdot T \cdot K_2\left(\frac{mc^2}{kT}\right) \quad (9)$$

where  $n$  is the particle density and  $K_2$  the modified Bessel function. The specific relation (9) between the spatial changes of density and temperature is due to the fact that in a general relativistic Boltzmann gas in collision-dominated equilibrium the chemical potential  $\mu$  divided by  $T$  is spatially constant. We note explicitly that (9) is not an equation of state. It describes exclusively the spatial changes of density and temperature in an equilibrium solution of Boltzmann's equation.

In the range of low temperatures  $kT \ll mc^2$  an asymptotic expansion of  $K_2$  yields

$$\varrho = const \cdot T^{3/2} \cdot \exp\left[-\frac{mc^2}{kT}\right] \quad (10)$$

This extremely sensitive exponential relation between the spatial changes of density and temperature has been found also by Dehnen and Obregon [8] in a quite different way.

The metric is determined by the field equations. We consider small anisotropies of the temperature, that means

$$T = T_1[1 + \tau(x^1, x^2, x^3)] \quad (11)$$

$$T_1 = const, \quad |\tau(x^1, x^2, x^3)| \ll 1$$

Furthermore we assume the gravitational field to be weak in the sense

$$g_{ik} = \eta_{ik} + h_{ik}(x^1, x^2, x^3)$$

$$\eta_{ik} = diag(1, 1, 1, -1) \quad (12)$$

$$|h_{ik}(x^1, x^2, x^3)| \ll 1$$

Starting from eqs. (11) and (12) the author has given a detailed analysis of the linearized field equations (with zero cosmological constant) in his previous paper [4]. From this analysis follows the basic equation

$$\Delta\tau = -\kappa_0 \left\{ \frac{1}{2} \varrho_1 c^2 \exp\left[-\frac{mc^2}{kT_1}(1 - \tau)\right] + aT_1^4 \right\} \quad (13)$$

where  $\Delta$  is the Laplacian,  $\kappa_0 = 8\pi G/c^4$  Einstein's gravitational constant and  $a = 7,564 \cdot 10^{-15} \text{ erg} \cdot \text{cm}^{-3} \cdot \text{K}^{-4}$  the black-body constant. Eq. (13) is for given background temperature  $T_1$  and some start value  $\varrho_1$  of the density a partial differential equation for the temperature anisotropies  $\tau$  in a general relativistic Boltzmann gas in collision-dominated equilibrium. The solution  $\tau$  determines then the density by means of

$$\varrho = \varrho_1 \exp \left[ -\frac{mc^2}{kT_1}(1 - \tau) \right] \quad (14)$$

Eq. (13) says that in a general relativistic Boltzmann gas in collision-dominated equilibrium anisotropies of the temperature must exist. Indeed, with  $\tau \equiv 0$  it follows from eq. (13) that  $\varrho_1 = 0$  and  $T_1 = 0$  and hence  $\varrho \equiv 0$  and  $T \equiv 0$ . The existence of these spatial fluctuations of temperature and density (by means of eq. (14)) is an intrinsically general relativistic effect. It is due to the coupling of the Boltzmann gas with the space-time metric via the field equations. In a special relativistic theory, however, space-time is fixed so that field equations do not exist. Then we have  $g_{44} = \text{const} = -1$  and hence  $T = \text{const}$  and  $\varrho = \text{const}$  according to eqs. (8) and (9). Because of  $mc^2/kT_1 \ll 1$  (later on we have  $m = m_p$  and  $T_1 \simeq 10^3 \text{ K}$  so that  $m_p c^2/kT_1 \simeq 10^{10}$ !) it follows from eq. (14) that smallest changes of  $\tau$  lead to extremely drastic changes of  $\varrho$ . Hence space-time is filled with sharply edged gas clouds although the temperature is nearly isotropic. This is the final state in the condensation process described later in section 4.2.

We are interested in a single gas cloud. Such a cloud is described by the equations (see ref. [4])

$$\left. \begin{aligned} \tau_c \Delta y &= -\frac{8\pi G}{c^4} \left\{ \frac{1}{2} \varrho_c c^2 \exp \left[ -\frac{mc^2 \tau_c}{kT_1}(1 - y) \right] + aT_1^4 \right\} \\ y &= \frac{\tau}{\tau_c} \leq 1, \quad y_c = y(0, 0, 0) = 1 \end{aligned} \right\} \quad (15a)$$

$$\varrho = \varrho_c \exp \left[ -\frac{mc^2 \tau_c}{kT_1}(1 - y) \right] \quad (15b)$$

Here the centre of the cloud is placed in the origin of the spatial coordinate system, and  $\varrho_c$  and  $\tau_c$  are the values of  $\varrho$  and  $\tau$  in the centre.

Again we emphasize that the density-temperature relation (10) or (15 b) holds in the final quasi-equilibrium state. The dynamical process ending in this final state will be treated below in section 4.2.

## 4. Galaxy formation

### 4.1 The cosmological background

Before describing in section 4.2 the galaxy formation as a sudden condensation process we lay out the cosmological model in which this process runs. In fig. 1 the age  $t_u$  of the universe depending on the present day density  $\varrho_0$  and the Hubble-parameter  $H_0 = h \cdot \text{km/secMpc}$  is plotted where  $h = 0$  marks the flat universe. The underlying cosmological model is a standard model with zero cosmological constant.

The recent controversy about the Hubble-parameter between Sandage/Tammann (small value of  $h$ ) and Freedman et al. (large value of  $h$ ) seems to end in a mean value  $h \simeq 70$ .

Furthermore the earlier large age of the globular clusters of about  $16 \cdot 10^9 y$  has been recently revised to  $(12 \pm 2) \cdot 10^9 y$  [9, 10]. So assuming a density  $\varrho_{0,L} \simeq 2 \cdot 10^{-31} g \cdot cm^{-3}$  of the luminous matter and taking into account the dark matter by a factor 5 to 10 we have a present day density  $\varrho_0 \simeq 10^{-30} g \cdot cm^{-3}$ . From fig. 1 we then read an age of the universe between  $12 \cdot 10^9 y$  and  $13 \cdot 10^9 y$  which is compatible with the age of the globular clusters. So all is right. However, a flat universe as predicted by an inflationary scenario in the very early universe seems to be ruled out. Obviously we are living in an open universe.

The line element of an open standard model in quasi-cartesian coordinates reads

$$ds^2 = \frac{1}{\left[1 - \frac{1}{4R^2(t)} \sum_{\alpha} (x^{\alpha})^2\right]^2} \left[ (dx^1)^2 + (dx^2)^2 + (dx^3)^2 \right] - \underbrace{(dx^4)^2}_{c^2 dt^2} \quad (16)$$

(greek indices running from 1 to 3). From the field equations with zero cosmological constant we obtain then in the matter-dominated era ( $T < T_{rek} = 3 \cdot 10^3 K$ )

$$ct = R \left\{ \left(1 + \frac{K}{R}\right)^{\frac{1}{2}} - \frac{1}{2} \frac{K}{R} \ln \left[ \frac{(1 + K/R)^{\frac{1}{2}} + 1}{(1 + K/R)^{\frac{1}{2}} - 1} \right] \right\} \quad (17a)$$

with

$$K = \frac{1}{3} \kappa_0 c^2 \varrho_0 R_0^3, \quad R_0 = (H_0^2 - \frac{1}{3} \kappa_0 c^2 \varrho_0)^{-\frac{1}{2}} \quad (17b)$$

and where the index  $_0$  denotes the present day values. In the temperature range  $T \gtrsim 10^3 K$  equation (17a) can be well approximated by

$$ct = \frac{1}{2K^{\frac{1}{2}}} R^{\frac{3}{2}} \quad (18)$$

From this equation we obtain

$$R = (2cK^{\frac{1}{2}})^{\frac{2}{3}} t^{\frac{2}{3}} \quad (19)$$

and furthermore by use of  $R \cdot T = \text{const}$  and eq. (17 b)

$$t = \frac{1}{2c^2} \left( \frac{3}{\kappa_0 \varrho_0} \right)^{\frac{1}{2}} \left( \frac{T_0}{T} \right)^{\frac{3}{2}} \quad (20)$$

with the present day temperature  $T_0 = 2,7 K$  of the background radiation.

## 4.2 The condensation process

In section 2 we realized that the cosmic matter gas runs from the end of recombination into a state very close to collision-dominated equilibrium. We describe this state in a very good approximation by the exact equilibrium as outlined in section 3. The single sharply edged gas clouds are then described by eqs. (15) where we consider the cosmic matter as a one-component gas with particle mass  $m_p$ . Below we shall find that the temperature in this state is about  $10^3 K$ . Then we have even for  $\tau_c \simeq 10^{-5}$  (COBE) in the exponent of the density (15 b) the enormous factor

$$\frac{m_p c^2 \tau_c}{k T_1} \simeq 10^5 \quad (21)$$

Hence, when  $y$  drops only a very little below 1, say  $y = 0,999$ , the density falls practically to zero.

Now we turn to the question how this process runs and how much time it takes. Clearly, the general relativistic Boltzmann equation

$$p^i \frac{\partial f}{\partial x^i} - \Gamma_{jk}^i p^j p^k \frac{\partial f}{\partial p^i} = \mathcal{C}(f) \quad (22)$$

determines this process. There is no hope to solve this equation unless we make some simplifications. Firstly we approximate the collision term  $\mathcal{C}(f)$  by the BGK-model [ 11 – 19 ]

$$\mathcal{C}(f) = -\frac{m_p}{t_c}(f - f_0) \quad (23)$$

where  $t_c$  is the mean time between two collisions as in section 2 and  $f_0$  is the distribution in collision-dominated equilibrium. Secondly we calculate the gravitational field  $\Gamma_{jk}^i$  only by means of the cosmological background (16). This means

$$\Gamma_{\alpha\beta}^\gamma|_{x=0} = 0$$

$$\Gamma_{\beta 4}^\alpha = \frac{1}{c} \frac{\dot{R}}{R} \delta_\beta^\alpha, \quad \Gamma_{44}^\alpha = 0 \quad (24)$$

$$\Gamma_{\alpha\beta}^4 = \frac{1}{c} \dot{R} R \delta_{\alpha\beta}, \quad \Gamma_{\alpha 4}^4 = 0 = \Gamma_{44}^4$$

where a dot denotes derivative with respect to  $t$  and  $x = 0$  means  $x^1 = x^2 = x^3 = 0$ . We suppose that at the end of recombination small anisotropies of the background radiation are left from processes in the very early universe and consider the regions where the above normalized temperature variable  $y$  is below 1. In these regions the later (quasi)-equilibrium distribution  $f_0$  approximately vanishes because the particle density is practically zero (see above). Furthermore we assume that in these regions

$$f = f(t, p^1, p^2, p^3) \quad (25)$$

where the spatial momentum components  $p^\alpha$  are related with the 4-th component  $p^4$  by the mass-shell condition

$$g_{ij} p^i p^j = g_{\alpha\beta} p^\alpha p^\beta - (p^4)^2 = -m_p^2 c^2 \quad (26)$$

In the cosmological epoch under consideration ( $T \leq 3 \cdot 10^3 K, m = m_p$ ) we have

$$g_{\alpha\beta} p^\alpha p^\beta \ll m_p^2 c^2 \quad (27)$$

so that

$$p^4 = m_p c \quad (28)$$

Making use of the property (25) we can place the points we consider at the origin  $x = 0$ . Then the Boltzmann equation (22) reduces by means of the collision term (23) with  $f_0 = 0$  and the relations (24), (25) and (28) to

$$\frac{\partial f}{\partial t} - 2 \frac{\dot{R}}{R} p^\alpha \frac{\partial f}{\partial p^\alpha} = -\frac{f}{t_c} \quad (29)$$

Next we integrate eq. (29) over the mass-shell (26) using the integration element [6]

$$\pi = \frac{1}{p^4} \sqrt{-g} dp^1 dp^2 dp^3 = \frac{1}{p^4} \sqrt{-g} d^3 p \quad (30)$$

where  $g = \det g_{ij}$ . By means of the metric (16) we have

$$\pi|_{x=0} = R^3(t) \frac{d^3 p}{m_p c} \quad (31)$$

By use of

$$\int f \pi|_{x=0} = n(t) = \text{particle density} \quad (32)$$

the integration yields

$$\begin{aligned} \int \frac{\partial f}{\partial t} \pi|_{x=0} &= \int \frac{\partial f}{\partial t} R^3(t) \frac{d^3 p}{m_p c} \\ &= \frac{d}{dt} \int f R^3 \frac{d^3 p}{m_p c} - 3 \int f R^2 \dot{R} \frac{d^3 p}{m_p c} \\ &= \frac{d}{dt} \int f \pi|_{x=0} - 3 \frac{\dot{R}}{R} \int f \pi|_{x=0} \\ &= \dot{n} - 3 \frac{\dot{R}}{R} n \end{aligned}$$

and

$$\int p^\alpha \frac{\partial f}{\partial p^\alpha} \pi|_{x=0} = \frac{R^3}{m_p c} \underbrace{\int p^\alpha \frac{\partial f}{\partial p^\alpha} d^3 p}_{(*)} = -3 \int f \pi|_{x=0} = -3n$$

where we used in the integral (\*) Gau' theorem. Hence we arrive at

$$\dot{n} = - \left( \frac{1}{t_c} + 3 \frac{\dot{R}}{R} \right) n \quad (33)$$

The collision time  $t_c$  is given by

$$t_c = (n \cdot v_{th} \cdot \sigma)^{-1} \quad (34a)$$

with the thermal velocity

$$v_{th} = \left( \frac{3kT}{m_p} \right)^{\frac{1}{2}} \quad (34b)$$

and the cross section

$$\sigma = \pi r_c^2 \quad (34c)$$

( $r_c = 7a_0$  from eq. (2)). Furthermore it follows from eq. (19) that

$$\frac{\dot{R}}{R} = \frac{2}{3t} \quad (35)$$



Hence eq. (33) takes the form

$$\begin{aligned}\dot{n} &= - \left( \lambda_1 T^{\frac{1}{2}} n + \frac{2}{t} \right) n \\ \lambda_1 &= \pi r_c^2 \left( \frac{3k}{m_p} \right)^{\frac{1}{2}}\end{aligned}\tag{36}$$

From eq. (20) we derive

$$T = T_0 \left( \frac{3}{4c^4 \kappa_0 \varrho_0} \right)^{\frac{1}{3}} \frac{1}{t^{\frac{2}{3}}}\tag{37}$$

so that we obtain finally the differential equation

$$\begin{aligned}\dot{n} &= - \left( \frac{\lambda}{t^{\frac{1}{3}}} n + \frac{2}{t} \right) n \\ \lambda &= \pi r_c^2 \left( \frac{3kT_0}{m_p} \right)^{\frac{1}{2}} \left( \frac{3}{4c^4 \kappa_0 \varrho_0} \right)^{\frac{1}{6}}\end{aligned}\tag{38}$$

for the particle density  $n$  between the gas clouds. This density decreases on the one hand by collisions (first term in the paranthesis on the right hand side of eq. (38)) and on the other hand by the cosmological expansion (second term). Below we shall find that after recombination at first the collision term is greater than the expansion term by about eight orders of magnitude. However, this extreme superiority decreases very rapidly.

The process (38) starts at the end of recombination at  $T = T_{rek} = 3 \cdot 10^3 K$ . Considering universes with

$$\varrho_0 = \alpha \cdot 10^{30} gcm^{-3}; \quad \alpha = 0.5, 1, 2.5\tag{39}$$

we obtain from eq. (20) the initial time

$$t = t_{rek} = \alpha^{-\frac{1}{2}} \cdot 0,57 \cdot 10^6 y\tag{40}$$

The particle density at  $t = t_{rek}$  is given by  $n_{rek} = \varrho_{rek}/m_p$  where

$$\varrho_{rek} = \alpha \cdot \bar{\varrho}_{rek}, \quad \bar{\varrho} = 1,4 \cdot 10^{-21} gcm^{-3}\tag{41}$$

with  $\bar{\varrho}_{rek}$  the density at the end of recombination in an universe with  $\varrho_0 = 10^{-30} gcm^{-3}$ . Hence we have the initial particle density

$$n = n_{rek} = \alpha \cdot 8,2 \cdot 10^2 cm^{-3}\tag{42}$$

Next we write the differential equation (38) in a dimensionless form by introducing

$$t = x \cdot 10^6 y, \quad n = \alpha \cdot \mu \cdot 8,2 \cdot 10^2 cm^{-3}\tag{43a}$$

with the initial values

$$x_{rek} = \alpha^{-\frac{1}{2}} \cdot 0,57, \quad \mu_{rek} = 1\tag{43b}$$

Then eq. (38) reads

$$\begin{aligned}\mu' &= \frac{d\mu}{dx} = -\left(\beta \frac{\mu}{x^{\frac{1}{3}}} + \frac{2}{x}\right)\mu \\ \beta &= \alpha^{\frac{5}{6}} \cdot 8,0 \cdot 10^7\end{aligned}\tag{44}$$

The substitution  $u = \mu^{-1}$  leads to the linear differential equation

$$u' = \frac{2}{x}u + \frac{\beta}{x^{\frac{1}{3}}}\tag{45}$$

with the general solution

$$u(x) = Cx^2 - \frac{3}{4}\beta x^{\frac{2}{3}}\tag{46}$$

The constant C is determined by the initial condition  $\mu(x_{rek}) = 1$  Hence we arrive at

$$\mu(x) = \left[ (x_{rek}^{-2} + \frac{3}{4}\beta x_{rek}^{-\frac{4}{3}})x^2 - \frac{3}{4}\beta x^{\frac{2}{3}} \right]^{-1}\tag{47}$$

For  $x$  well larger than  $x_{rek}$  this solution can be written in the form

$$\mu(x) = \frac{4}{3\beta} \frac{1}{x^2 \left( x_{rek}^{-\frac{4}{3}} - x^{-\frac{4}{3}} \right)}\tag{48}$$

The dimensionless form (44) of the differential equation (38) shows the enormous collision rate (first term in the parantheses on the right hand side) just after recombination.

We suppose that the process of cloud formation is worked out when the cosmological expansion rate predominates more or less strongly the collision rate. Hence we determine the end  $x_1$  of the condensation process by

$$\frac{2}{x_1} = b \beta \frac{\mu(x_1)}{x_1^{\frac{1}{3}}}, \quad b \simeq 10\tag{49}$$

which by means of the solution (48) yields

$$x_1 = \left( \frac{2}{3}b + 1 \right)^{\frac{3}{4}} x_{rek}\tag{50}$$

From eq. (50) we obtain the cosmological instant

$$t_1 = \left( \frac{2}{3}b + 1 \right)^{\frac{3}{4}} \alpha^{-\frac{1}{2}} \cdot 0,57 \cdot 10^6 y\tag{51}$$

of the end of the condensation process, its duration

$$\Delta t = \left[ \left( \frac{2}{3}b + 1 \right)^{\frac{3}{4}} - 1 \right] 0,57 \cdot \alpha^{-\frac{1}{2}} \cdot 10^6 y\tag{52}$$

and by use of eq. (37) the temperature

$$T_1 = T_{rek} \left( \frac{x_{rek}}{x_1} \right)^{\frac{2}{3}} = \left( \frac{2}{3}b + 1 \right)^{-\frac{1}{2}} T_{rek} \quad (53)$$

Finally we obtain from eq. (49) the value

$$\mu_1 = \mu(x_1) = \frac{3,6 \cdot 10^{-8}}{b \left( \frac{2}{3}b + 1 \right)^{\frac{1}{2}} \cdot \alpha^{\frac{1}{2}}} \quad (54)$$

In tables 1 and 2 we give for  $b = 10$  and  $b = 20$  the values of  $t_1, \Delta t, \mu_1$  and  $T_1$  where  $\alpha$  runs through the values according to eq. (39).

The last row in table 1 gives the ratio  $\frac{1}{2}c\Delta t/R_1$  where  $R_1 = R(t_1)$  and  $R(t_1)$  is calculated from eq. (19) by use of a mean Hubble-parameter  $h = 70$ . In section 4.3 we shall consider axially symmetric gas clouds. The maximal linear extension of these clouds is  $c\Delta t$  because the clouds must be causally connected. From the centre of the clouds to the edge we have then a maximal extension  $\frac{1}{2}c\Delta t$ . This length must be much smaller than  $R_1$  otherwise the weak field expansion (12) does not hold (see the line element (16)).

#### 4.3 The mass spectrum

We can be sure that protogalaxies had been axially symmetric objects with their lower limit of spherically symmetric globular clusters. Hence we are interested in axially and spherically symmetric solutions of the single-cloud equations (15).

We fix the particle mass as above by  $m = m_p$  and let the anisotropies  $\tau_c$  of the temperature vary in the range

$$10^{-4} \geq \tau_c \geq 10^{-7} \quad (55)$$

The background temperature  $T_1$  is determined by the parameter  $b$  (see tables 1 and 2). What about the density  $\varrho_c$  in the centre? In section 4.2 we established that the condensation process, that means the formation of the very sharp edges of the gas clouds, runs very rapidly. Furthermore the linear extension of the clouds is much smaller than the curvature radius  $R$ . Thus the clouds are not subject to the cosmic expansion and hence we can assume

$$\varrho_c = \varrho_{rek} = \alpha \bar{\varrho}_{rek} \quad (56)$$

with  $\varrho_{rek}$  and  $\bar{\varrho}_{rek}$  according to eq. (41). As in the previous papers [3,4] we introduce

$$\frac{1}{l_{rek}^2} = \frac{8\pi G}{c^2} \bar{\varrho}_{rek}, \quad l_{rek} = 6,6 \cdot 10^5 ly \quad (57)$$

and the dimensionless variable

$$\bar{x}^\alpha = \frac{1}{\sqrt{\tau_c} l_{rek}} x^\alpha \quad (58)$$

Then eqs. (15) take the form

$$\left. \begin{aligned} \Delta_{\bar{x}} y &= -\alpha_1 \exp \left[ -\frac{m_p c^2 \tau_c}{k T_1} (1 - y) \right] - q \\ y &\leq 1, \quad y(0, 0, 0) = 1 \\ \alpha_1 &= \frac{1}{2} \alpha, \quad q = a T_1^4 / \bar{\varrho}_{rek} c^2 \end{aligned} \right\} \quad (59a)$$

$$\varrho = \alpha \bar{\varrho}_{rek} \exp \left[ -\frac{m_p c^2 \tau_c}{k T_1} (1 - y) \right] \quad (59b)$$

where  $\Delta_{\bar{x}}$  denotes the Laplacian with respect to  $\bar{x}^\alpha$ .

#### 4.3.1 Spherically symmetric clouds

We denote the dimensionless radial coordinate by  $x$  so that  $y = y(x)$ . Then eq. (59a) reads

$$y'' + \frac{2}{x} y' = -\alpha_1 \exp \left[ -\frac{m_p c^2 \tau_c}{k T_1} (1 - y) \right] - q \quad (60a)$$

$$y(0) = 1 \quad (60b)$$

To the natural boundary condition  $y(0) = 1$  we add the regularity condition

$$y'(0) = 0 \quad (60c)$$

In his previous paper [3] the author investigated the differential equation (60) in detail. It turned out that the natural boundary condition (60b) implies the regularity (60c). The solution takes in the very vicinity of the centre the form

$$\begin{aligned} y_i(x) &= 1 - \frac{\alpha_1 + q}{\beta} + \frac{\alpha_1 + q}{\beta^{\frac{3}{2}} x} \sin(\beta^{\frac{1}{2}} x) \\ \beta &= \frac{m_p c^2 \tau_c \alpha_1}{k T_1} \end{aligned} \quad (61)$$

This solution is used as start for a numerical integration of eq. (60a) by a Range-Kutta-method.

The mass  $M$  of the gas clouds in the centre of the anisotropies is given by

$$M = 4\pi \int_0^{r_1} \varrho r^2 dr, \quad r = \sqrt{\tau_c} l_{rek} x \quad (62)$$

with the density  $\varrho$  according to eq. (59 b). In section 4.2 we have shown that the particle density at the boundary of the clouds drops to  $\mu_1 n_{rek}$  when the condensation process is closed. Hence  $r_1$  in the mass integral (62) is strictly speaking given by  $\varrho(r_1) = \mu_1 \varrho_c$  (see eq. (56)). However, the numerical calculations show that the masses practically do not change if we fix  $r_1$  by  $\varrho(r_1) = 10^{-5} \varrho_c$ . This is due to the extremely rapid decrease of  $\varrho$ .

Writing the mass formula (62) in a dimensionless form we obtain

$$\frac{M}{M_\odot} = 2,13 \cdot 10^{18} \cdot \alpha \cdot \tau_c^{\frac{3}{2}} \int_0^{x_1} \exp[-\gamma(1 - y(x))] x^2 dx \quad (63)$$

$$\gamma = \frac{m_p c^2 \tau_c}{k T_1}, \quad \exp[-\gamma(1 - y(x_1))] = 10^{-5}$$

The integral in eq. (63) can be easily evaluated by use of the numerical solution  $y(x)$ . In tables 3 and 4 the results are listed where  $D = 2r_1$  is the diameter of the clouds. All results are independent of the central value  $\tau_c$  in the range (55). Finally we note that the radii  $\frac{1}{2}D$  of the clouds are very much smaller than  $R_1$  (see the end of section 4.2).

#### 4.3.2 Axially symmetric clouds

We introduce dimensionless cylindrical coordinates  $x$  (distance from the symmetry axis) and  $\zeta$  ( $z$ -coordinate) so that  $y = y(x, \zeta)$ . Then eq. (59 a) reads

$$\frac{\partial^2 y}{\partial x^2} + \frac{1}{x} \frac{\partial y}{\partial x} + \frac{\partial^2 y}{\partial \zeta^2} = -\alpha_1 \exp[-\gamma(1 - y)] - q \quad (64a)$$

with  $\gamma$  according to eq. (63). Again we have the natural boundary condition

$$y(0, 0) = 1 \quad (64b)$$

and the regularity condition

$$\frac{\partial y}{\partial x}(0, \zeta) = 0 = \frac{\partial y}{\partial \zeta}(x, 0) \quad (64c)$$

Also the partial differential equation (64) has been investigated in detail by the author in his previous paper [3]. The solution is composed of an interior solution

$$y_i(x, \zeta) = 1 - \frac{1}{2}(\alpha_1 + q) \left[ \frac{1}{2} C x^2 + (1 - C) \zeta^2 \right], \quad (65a)$$

an exterior solution (when the density term on the right hand side of eq. (64 a) has practically fallen to zero)

$$y_a(x, \zeta) = 1 - \frac{1}{2} q \left[ \frac{1}{2} C x^2 + (1 - C) \zeta^2 \right] \quad (65b)$$

and a fit function

$$y_f(x, \zeta) = 1 + \epsilon - \sqrt{2\epsilon(\alpha_1 + q)} \sqrt{\frac{1}{2} C x^2 + (1 - C) \zeta^2}, \quad \epsilon \ll 1 \quad (65c)$$

with a flattening parameter  $C$  in the range

$$0 < C < 1 \quad (65d)$$

The fit function connects the interior and exterior solution. It is fit smoothly to the interior solution on a surface  $y_i(x, \zeta) = 1 - \epsilon = \text{const.}$  i.e.

$$\frac{1}{2} C x^2 + (1 - C) \zeta^2 = \frac{2\epsilon}{\alpha_1 + q} \quad (66)$$

and intersects the exterior solution on the surface

$$\frac{1}{2}Cx^2 + (1-C)\zeta^2 = \frac{2\epsilon}{q^2}(\sqrt{\alpha_1+q} + \sqrt{\alpha_1})^2 \quad (67)$$

The solution is spherically symmetric for  $C = \frac{2}{3}$ . Then the interior solution (65 a) reads

$$y_i(x, \zeta) = 1 - \frac{1}{6}(\alpha_1 + q)(x^2 + \zeta^2) \quad (68)$$

which agrees with the spherically symmetric solution (61) if one takes the first two terms in the expansion of the sin.

On the surface of intersection (67) the density term on the right hand side of eq. (64 a) has the value

$$\alpha_1 \exp[-\gamma(1 - y_a)] = \alpha_1 \exp\left[-\frac{\gamma\epsilon}{q}(\sqrt{\alpha_1+q} + \sqrt{\alpha_1})^2\right] = \epsilon_1 \quad (69)$$

We express the parameter  $\epsilon$  in terms of  $\epsilon_1$  and obtain

$$\epsilon = -\frac{q \ln(\epsilon_1/\alpha_1)}{\gamma(\sqrt{\alpha_1+q} + \sqrt{\alpha_1})^2} \quad (70)$$

Now we determine for given  $T_1(\leadsto q, \gamma)$  and  $\alpha_1$  the parameter  $\epsilon$  by fixing  $\epsilon_1$  such that the mass integral for  $C = \frac{2}{3}$  (spherical symmetry) agrees with the spherically symmetric masses calculated in section 4.3.1. As above we have the dimensionless mass formula

$$\frac{M}{M_\odot} = 2,13 \cdot 10^{18} \cdot \alpha \cdot \tau_c^{\frac{3}{2}} \int_0^{x_1} \int_0^{\zeta_1} \exp[-\gamma(1 - y(x, \zeta))] x dx d\zeta \quad (71a)$$

where again at the upper limits of the integral the density has fallen to  $10^{-5}\varrho_c$ , *i.e.*

$$\exp[-\gamma(1 - y(x_1, 0))] = 10^{-5} = \exp[-\gamma(1 - y(x, \zeta_1))], \quad x \leq x_1 \quad (71b)$$

and  $y(x, \zeta)$  is the composed solution (65).

In tables 5 and 6 the values of  $\epsilon_1$  are listed where we listed for reasons of later comparison in the last row the values of  $\mu_1$  (see eq. (54)). Again the values of  $\epsilon_1$  do not depend on  $\tau_c$  (the values of  $\epsilon$ , therefore, depend on  $\tau_c$  since  $\gamma$  depends on  $\tau_c$ ).

For  $C \rightarrow 0$  and  $C \rightarrow 1$  the clouds are pancake-like and cigar-like respectively (see fig. 2). We note that these configurations exist in an exact equilibrium state in the global rest frame (see section 3), especially the pancakes do not rotate. They are hold by a complicated balance of pressure and gravitational forces where the gravitational forces come also from the radiation field [4].

What are the minimal and maximal value of  $C$ ? We know from section 4.2 and eq. (56) that at the end of the condensation process the density at the boundary of the clouds drops to  $\mu_1\varrho_c$ . Hence we obtain from eqs. (59 b), (56) and (58) a relation between the flattening parameter  $C$  and the semiaxes  $r_0$  and  $z_0$  by means of

$$\exp[-\gamma(1 - y(x_0, 0))] = \mu_1 = \exp[-\gamma(1 - y(0, \zeta_0))] \quad (72)$$

$$x_0 = \frac{r_0}{\sqrt{\tau_c} l_{rek}}, \quad \zeta_0 = \frac{z_0}{\sqrt{\tau_c} l_{rek}}$$

From tables 5 and 6 we see that  $\epsilon_1/\alpha_1 \ll \mu_1$ . According to eq. (69) this means that the exponential is on the surface of intersection between the fit function and the exterior solution very much smaller than  $\mu_1$ . Hence  $y$  in eq. (72) lies in the domain of  $y_f$ . By use of eqs. (65 c) and (70) we obtain then from eq. (72)

$$\left. \begin{array}{l} \frac{r_0 \sqrt{C}}{l_{rek}} \\ \frac{z_0 \sqrt{2(1-C)}}{l_{rek}} \end{array} \right\} = -0,96 \cdot 10^{-5} (T_1 [10^3 K])^{\frac{1}{2}} \left\{ \ln \mu_1 + \frac{q \ln(\epsilon_1/\alpha_1)}{(\sqrt{\alpha_1 + q} + \sqrt{\alpha_1})^2} \right\} \cdot \frac{\sqrt{\alpha_1 + q} + \sqrt{\alpha_1}}{[-q(\alpha_1 + q) \ln(\epsilon_1/\alpha_1)]^{\frac{1}{2}}} \quad (73)$$

Since the clouds must be causally connected at the end of the condensation process the semiaxes  $r_0$  for  $C \rightarrow 0$  and  $z_0$  for  $C \rightarrow 1$  are limited by

$$2r_{0,max} = c\Delta t = 2z_{0,max} \quad (74)$$

where  $\Delta t$  is the duration of the condensation process according to tables 1 and 2. With these upper limits of  $r_0$  and  $z_0$  we calculate from eq. (73) the values  $C_{min}$  and  $C_{max}$ . The results are listed in tables 7 and 8.

With the composed solution (65) we can now easily compute from the mass formula (71) the masses of the clouds for given flattening parameters  $C$  where again it is sufficient to break off the integration when the density drops to  $10^{-5} \rho_c$  (instead of  $\mu_1 \rho_c$ ). The results are listed in tables 9 and 10. Again all is independent of the central value  $\tau_c$  in the range (55).

The mass spectrum we obtained is rather satisfactory. In fact, it shows the observed upper limit masses  $M \simeq 10^{12} M_\odot$  as well as the lower limit masses  $M \simeq 10^5 M_\odot$  where, beyond it, the lower limit masses are spheres. However, the upper limit masses  $M \simeq 10^{12} M_\odot$  are extremely thin pancakes, and galaxies are not observed in this form. Thus we investigate in the following section the evolution of the condensation "drops" where we argue as in the author's previous paper [3].

##### 5) The evolution of the clouds after the condensation process

After the condensation "drops" have formed a few  $10^6$  years after the big bang the universe cools further down, that means, the background temperature  $T_1$  decreases. If we assume that the quasi-equilibrium at first stands we conclude from eq. (73) that the semiaxes  $r_0$  and  $z_0$  change by means of  $T_1^{\frac{1}{2}}$  in front of the curly bracket and  $q \sim T_1^4$  (see eq. (59a)). The second

term in the curly bracket can be neglected against  $ln\mu_1$  and hence we have approximately

$$r_0 \sim \frac{1}{T_1^{\frac{3}{2}}}, z_0 \sim \frac{1}{T_1^{\frac{3}{2}}} \quad (75)$$

This means that the density  $\varrho_{cl}$  in the clouds decreases as

$$\varrho_{cl} \sim T_1^{\frac{9}{2}} \quad (76)$$

Then the characteristic expansion time of the clouds is given by

$$\tau_{\text{exp}} = \left| \frac{\varrho_{cl}}{\dot{\varrho}_{cl}} \right| = \frac{2}{9} \left| \frac{T_1}{\dot{T}_1} \right| = \frac{2}{9} \frac{R}{\dot{R}} \quad (77)$$

where we used the cosmological law  $R \cdot T = \text{const}$ . We compare this characteristic time with the mean time  $\tau_{\text{coll}}$  between two collisions of particles in the clouds. It is given by

$$\tau_{\text{coll}} = (n_{cl} \cdot v_{th} \cdot \sigma)^{-1} \quad (78a)$$

with the particle density

$$n_{cl} = \frac{\varrho_{cl}}{m_p} \quad (78b),$$

the thermal velocity

$$v_{th} = \left( \frac{3kT_1}{m_p} \right)^{\frac{1}{2}} \quad (78c)$$

and the cross section

$$\sigma = \pi r_c^2 \quad (78d)$$

(see eq. (34)). According to eq. (76) the density  $\varrho_{cl}$  can be written in the form

$$\varrho_{cl} = \varrho_{cl,1} \left( \frac{T_1}{10^3 K} \right)^{\frac{9}{2}} \quad (79a)$$

where we use a mean value  $T_1 = 10^3 K$  at the end of the condensation process and hence

$$\varrho_{cl,1} \simeq \alpha \cdot 10^{-21} g \cdot cm^{-3} \quad (79b)$$

(see eq. (41)). In eq. (77) we use the field equation

$$\frac{R}{\dot{R}} \simeq \frac{1}{c^2} \left( \frac{3}{\kappa_o \varrho} \right)^{\frac{1}{2}} \quad (80)$$

with the mean cosmological density  $\varrho$  which is correlated to the background temperature  $T_1$  by means of  $\varrho \sim T_1^3$ . Hence we have

$$\varrho = \varrho_1 \left( \frac{T_1}{10^3 K} \right)^3 \quad (81a)$$

with the cosmological density  $\varrho_1$  at  $T_1 = 10^3 K$  given by

$$\varrho_1 = \left( \frac{1}{3} \right)^3 \alpha \bar{\varrho}_{rek} = \alpha \cdot 5 \cdot 10^{-23} gcm^{-3} \quad (81b)$$



Sticking all together we find

$$\frac{\tau_{coll}}{\tau_{exp}} \simeq \alpha^{-\frac{1}{2}} \cdot 2 \cdot 10^{-8} \left( \frac{10^3 K}{T_1} \right)^{\frac{7}{2}} \quad (82)$$

This relation tells us that the clouds when expanding run rather rapidly out of their quasi-equilibrium state so that the contraction due to the decreasing temperature begins. We assume that the two effects nearly cancel so that the clouds after the condensation process at first simply drift apart until the universe has cooled down drastically, say down to  $T \simeq 100K = T_2$ . At this time the universe is about  $10^8 y$  old and we assume that the clouds begin to contract.

We consider this contraction in more detail. Especially we are interested in the upper limit masses  $M \simeq 10^{12} M_\odot$  which are extremely thin pancakes. Indeed, with  $C \simeq 10^{-7}$  (see tables 7 to 10) we obtain from eq. (73)

$$\frac{z_o}{r_o} = \sqrt{\frac{C}{2(1-C)}} \simeq \frac{1}{4500} \quad (83)$$

How do these clouds contract? To answer this question we compare the gravitational energy  $E_G$  of the clouds with their thermal energy  $E_{th}$  after they have drifted apart and the universe has cooled down to  $T_2 \simeq 100K$ . We have

$$E_G \simeq -\frac{GM^2}{V^{\frac{1}{3}}}, \quad E_{th} \simeq P \cdot V, \quad P \simeq \frac{\bar{\rho} k T_2}{m_p} \quad (84a)$$

with the volume  $V$  of the clouds and a nearly constant density

$$\bar{\rho} \simeq \alpha \bar{\rho}_{rek} \simeq \alpha \cdot 10^{-21} gcm^{-3} \quad (84b)$$

From these equations we obtain

$$|E_G| \simeq \frac{Gm_p \bar{\rho}^{\frac{1}{3}} M_\odot^{\frac{2}{3}}}{kT_2} \left( \frac{M}{M_\odot} \right)^{\frac{2}{3}} E_{th} \simeq 10^{-2} \alpha^{\frac{1}{3}} \left( \frac{M}{M_\odot} \right)^{\frac{2}{3}} E_{th} \quad (85)$$

which yields for the upper limit masses  $M \simeq 10^{12} M_\odot$

$$|E_G| \simeq 10^6 E_{th} \quad (86)$$

Hence we conclude that the semimajor axis of the upper limit clouds decrease in a rough approximation like a freely falling particle according to

$$\ddot{r}(t) = -\frac{GM}{r^2(t)} \quad (87a)$$

with the initial conditions

$$r(0) = r_1, \quad \dot{r}(0) = 0 \quad (87b)$$

Here we use the initial value  $r(0) = r_1$  with  $r_1$  according to eqs. (63) and (71) since the mass outside of  $r_1$  is negligible. The solution of eq. (87) reads

$$\sqrt{2GM} t = r_1^{\frac{3}{2}} \left[ \arctg \sqrt{\frac{r_1}{r} - 1} + \sqrt{\frac{r}{r_1}} \sqrt{1 - \frac{r}{r_1}} \right] \quad (88)$$

With increasing contraction the cloud begins to rotate so that the contraction will be retarded until it stops at a final radius  $r_2$ . We approximate the contraction time  $t_{contr}$  by

$$t_{contr} = 2t_f \quad (89)$$

where  $t_f$  is the free fall time (88) when  $r = \frac{1}{2}(r_1 + r_2)$ .

We calculate the contraction times explicitly in an universe with  $\varrho_0 = 10^{-30} gcm^{-3} (\alpha = 1)$  for  $b = 10$  (see table 9). For  $C = C_{min}$  we have  $M = 6,6 \cdot 10^{11} M_\odot$  which might be our galaxy including dark matter. We obtain the initial value  $r_1$  from eq. (73) by replacing  $\mu_1$  by  $10^{-5}$  (see eq. (71)). We find

$$r_1 = 6,0 \cdot 10^5 ly \quad (90)$$

For the final value  $r_2$  we take the present day value of our galaxy, hence

$$r_2 = 0,5 \cdot 10^5 ly \quad (91)$$

Then we obtain a contraction time

$$t_{contr} = 2,5 \cdot 10^9 y \quad (92)$$

Calculating the red shift

$$z = \frac{R_0}{R} - 1 \quad (93)$$

corresponding to the time (92) from eq. (17) by use of a Hubble-parameter  $h = 70$  we find

$$z \simeq 3 \quad (94)$$

Let us consider the same galaxy at the earlier time  $t = 0,5t_{contr}$ . At this time the radial flow velocities  $v$  of matter are extremely high. From eq. (87) we obtain

$$v(r) = \sqrt{2GM} \sqrt{\frac{1}{r} - \frac{1}{r_1}} \quad (95)$$

which for  $r = \frac{1}{2}(r_1 + r_2) (t = t_f = 0,5t_{contr})$  yields

$$v \simeq 10^7 cm/sec \quad (96)$$

Comparing this velocity with the velocity of sound

$$c_s = \left( \frac{kT}{m_p} \right)^{\frac{1}{2}} \quad (97)$$

for  $T \simeq 300K$  we find

$$v \simeq 10^2 c_s \quad (98)$$

Hence at the earlier time  $t = 0,5t_{contr}$  the galaxy is in a highly active state where the redshift corresponding to this time is

$$z \simeq 5,8 \quad (99)$$

Next we consider in table 9 the parameter  $C = 10^{-2}$  with a mass  $M = 10^7 M_\odot$  which is the upper limit of globular clusters. We have the ratio

$$\frac{z_0}{r_0} = \frac{1}{14} \quad (100)$$

and from eq. (85)

$$|E_G| \simeq 500 E_{th} \quad (101)$$

We calculate the contraction time as above where we assume that the contraction stops when the mass has become a sphere. Then we obtain

$$t_{contr} = 1,6 \cdot 10^8 y \quad (102)$$

However, doing the same for  $C = 0,9999$  with again  $M \simeq 10^7 M_\odot$  we find

$$\frac{z_0}{r_0} = 71 \quad (103)$$

and a contraction time

$$t_{contr} = 3 \cdot 10^9 y \quad (104)$$

Finally we obtain for  $C = 0,999999$  with a mass  $M \simeq 10^8 M_\odot$  the ratio

$$\frac{z_0}{r_0} = 707 \quad (105)$$

and the enormous contraction time

$$t_{contr} = 30 \cdot 10^9 y \quad (106)$$

## 6) Conclusion

Obviously our results agree very well with observations. The upper limit masses  $M \simeq 10^{12} M_\odot$  evolve to fastly rotating spiral galaxies and are ready for the evolution of stars about  $2,5 \cdot 10^9 y$  after the big bang. They are observed in their final state with a redshift  $z \simeq 3$  and in an earlier highly active state with a redshift  $z \simeq 5$ . The lower limit masses  $M \simeq 10^5 M_\odot$  are born as spheres and are therefore ready for the evolution of stars a few  $10^6$  years after the big bang. Hence the stars in globular clusters are very old in agreement with observations.

What about the cigar-like clouds for  $C \rightarrow 1$ ? Maybe they have never existed. However, provided they have existed their contraction time is too long to evolve into clouds which are more or less spherically symmetric. They rather become unstable and decay into irregular clouds. Are these clouds the dark matter?

Finally we discuss the fact that the masses of the clouds do not depend on the central value  $\tau_c$  in the range (55) (see section 4.3). First of all we note that the anisotropies must be axially symmetric only in the very inner region since the density of the clouds falls practically to zero when the variable  $y = \tau/\tau_c$  drops to  $y = 0,99$  (see eq. (59 b)). Hence an anisotropy  $\tau_c \simeq 10^{-5}$  can be composed of say 100 axially symmetric anisotropies  $\tau_c \simeq 10^{-7}$  and covers then about 100 galaxies. Thus the spatial pattern of anisotropies of the background radiation after recombination might have been composed of chains and slices and hence matter has been arranged in chains and slices of galaxies. To this initial pattern of galaxies the machinery used by the Virgo Consortium [2] can be applied to give the large scale structures we observe today. However, in contrast to the results by the Virgo Consortium the structures consist now of luminous matter.

## REFERENCES

- [1] S. Weinberg, Gravitation and Cosmology,  
J. Wiley, New York (1972)
- [2] Virgo Consortium (F. Pearce, P. Thomas, A. Jenkins,  
C. S. Frenk, H. Couchman, S. White, J. Colberg,  
G. Efstathiou, A. Nelson, J. Peacock),  
Annual Report 1995, Max–Planck–Institute Garching
- [3] G. Lessner, GRG 26 (1994), 385
- [4] G. Lessner, GRG 27 (1995), 417
- [5] G. Lessner, Astrophys. and Space Sci. 161 (1989), 175
- [6] J. M. Stuart, Cargse Lectures in Physics 6,  
E. Schatzman, ed., Gordon and Breach, New York (1973)
- [7] W. Israel, in General Relativity, L. O’Raifeartaigh, ed.  
Clarendon Press, Oxford (1972)
- [8] H. Dehnen, O. Obregon, Astron. and Astrophys. 12 (1971), 161
- [9] B. Chaboyer, Y.C. Kim, Ap. J. 454 (1995), 767
- [10] M. Salaris, S. Degl’Innocenti, A. Weiss, Ap. J. 479 (1997), 665
- [11] S. Chapman, T.G. Cowling, The Mathematical Theory of  
Non–Uniform Gases, Cambridge University Press, Cambridge (1970)
- [12] C. Cercignani, Theory and Application of the Boltzmann Equation,  
Scottish Academic Press, Edinburgh, London (1975)
- [13] C.Marle, Ann. Inst. H. Poincare 10 (1969), 67
- [14] J. D. Nightingale, Ap. J. 185 (1973), 105
- [15] J. L. Anderson, H. R. Witting, Physica 74 (1974), 466
- [16] J. L. Anderson, A. C. Payne, Physica 85 A (1976), 261
- [17] R. Dominguez–Tenreiro, R. Hakim, Phys. Rev. D 15 (1977), 1435
- [18] A. Majorana, J. Math. Phys. 31 (1990), 2042
- [19] F. P. Wolvaardt, R. Maartens, Class. Quant. Grav. 11 (1994), 203;  
14(1997), 535

| $\alpha$                   | 0.5                 | 1                   | 2                    | 5                    |
|----------------------------|---------------------|---------------------|----------------------|----------------------|
| $t_1[10^6 y]$              | 3,7                 | 2,6                 | 1,9                  | 1,2                  |
| $\Delta t[10^6 y]$         | 2,9                 | 2,1                 | 1,5                  | 0,92                 |
| $\mu_1$                    | $1,8 \cdot 10^{-9}$ | $1,3 \cdot 10^{-9}$ | $9,2 \cdot 10^{-10}$ | $5,8 \cdot 10^{-10}$ |
| $\frac{1}{2}c\Delta t/R_1$ | 0,04                | 0,03                | 0,02                 | 0,01                 |

Table 1: The values of  $t_1$ ,  $\Delta t$  and  $\mu_1$   
for  $b = 10$  ( $T_1 = 1,08 \cdot 10^3 K$ )

| $\alpha$           | 0.5                  | 1                    | 2                    | 5                    |
|--------------------|----------------------|----------------------|----------------------|----------------------|
| $t_1[10^6 y]$      | 5,9                  | 4,2                  | 3,0                  | 1,9                  |
| $\Delta t[10^6 y]$ | 5,1                  | 3,6                  | 2,6                  | 1,6                  |
| $\mu_1$            | $6,7 \cdot 10^{-10}$ | $4,8 \cdot 10^{-10}$ | $3,4 \cdot 10^{-10}$ | $2,1 \cdot 10^{-10}$ |

Table 2: The values of  $t_1$ ,  $\Delta t$  and  $\mu_1$   
for  $b = 20$  ( $T_1 = 0,792 \cdot 10^3 K$ )

| $\alpha$      | 0.5              | 1                | 2                | 5                |
|---------------|------------------|------------------|------------------|------------------|
| $M/M_{\odot}$ | $2,7 \cdot 10^5$ | $2,5 \cdot 10^5$ | $2,4 \cdot 10^5$ | $2,2 \cdot 10^5$ |
| D [ ly ]      | 870              | 820              | 770              | 700              |

Table 3: Masses M and diameters D of gas clouds in the centre if spherically symmetric anisotropies for  $b = 10$  ( $T_1 = 1,08 \cdot 10^3 K$ ,  $q = 0,0083$ )

| $\alpha$      | 0.5              | 1                | 2                | 5                |
|---------------|------------------|------------------|------------------|------------------|
| $M/M_{\odot}$ | $2,8 \cdot 10^5$ | $2,6 \cdot 10^5$ | $2,5 \cdot 10^5$ | $2,4 \cdot 10^5$ |
| D [ ly ]      | 1240             | 1160             | 1070             | 960              |

Table 4: Masses M and diameters D of gas clouds in the centre of spherically symmetric anisotropies for  $b = 20$  ( $T_1 = 0,792 \cdot 10^3 K$ ,  $q = 0,0024$ )

| $\alpha$        | 0.5                 | 1                   | 2                    | 5                    |
|-----------------|---------------------|---------------------|----------------------|----------------------|
| $\varepsilon_1$ | $6 \cdot 10^{-16}$  | $2 \cdot 10^{-24}$  | $10^{-38}$           | $10^{-71}$           |
| $\mu_1$         | $1,8 \cdot 10^{-9}$ | $1,3 \cdot 10^{-9}$ | $9,2 \cdot 10^{-10}$ | $5,8 \cdot 10^{-10}$ |

Table 5: The parameter  $\varepsilon_1$  for  $b = 10$   
 $(T_1 = 1,08 \cdot 10^3 K, q = 0,0083)$

| $\alpha$        | 0.5                  | 1                    | 2                    | 5                    |
|-----------------|----------------------|----------------------|----------------------|----------------------|
| $\varepsilon_1$ | $10^{-35}$           | $10^{-56}$           | $5 \cdot 10^{-90}$   | $10^{-164}$          |
| $\mu_1$         | $6,7 \cdot 10^{-10}$ | $4,8 \cdot 10^{-10}$ | $3,4 \cdot 10^{-10}$ | $2,1 \cdot 10^{-10}$ |

Table 6: The parameter  $\varepsilon_1$  for  $b = 20$   
 $(T_1 = 0,792 \cdot 10^3 K, q = 0,0024)$

| $\alpha$   | 0.5                  | 1                    | 2                    | 5                    |
|------------|----------------------|----------------------|----------------------|----------------------|
| $C_{\min}$ | $1,21 \cdot 10^{-7}$ | $1,50 \cdot 10^{-7}$ | $1,87 \cdot 10^{-7}$ | $2,75 \cdot 10^{-7}$ |
| $C_{\max}$ | 0,999999<br>939      | 0,999999<br>925      | 0,999999<br>906      | 0,999999<br>862      |

Table 7: The values of  $C_{\min}$   
and  $C_{\max}$  for  $b = 10$   
( $T_1 = 1,08 \cdot 10^3$  K,  $q = 0,0083$ )

| $\alpha$   | 0.5                  | 1                    | 2                    | 5                    |
|------------|----------------------|----------------------|----------------------|----------------------|
| $C_{\min}$ | $4,66 \cdot 10^{-8}$ | $5,95 \cdot 10^{-8}$ | $7,34 \cdot 10^{-8}$ | $1,10 \cdot 10^{-7}$ |
| $C_{\max}$ | 0,999999<br>976      | 0,999999<br>970      | 0,999999<br>963      | 0,999999<br>945      |

Table 8: The values of  $C_{\min}$   
and  $C_{\max}$  for  $b = 20$   
( $T_1 = 0,792 \cdot 10^3$  K,  $q = 0,0024$ )



| $C$       | $M/M_{\odot}(\alpha = 0, 5)$ | $M/M_{\odot}(\alpha = 1)$ | $M/M_{\odot}(\alpha = 2)$ | $M/M_{\odot}(\alpha = 5)$ |
|-----------|------------------------------|---------------------------|---------------------------|---------------------------|
| $C_{min}$ | $8,5 \cdot 10^{11}$          | $6,6 \cdot 10^{11}$       | $4,9 \cdot 10^{11}$       | $3,1 \cdot 10^{11}$       |
| $10^{-6}$ | $1.0 \cdot 10^{11}$          | $9,8 \cdot 10^{10}$       | $9,1 \cdot 10^{10}$       | $8,5 \cdot 10^{10}$       |
| $10^{-5}$ | $1.0 \cdot 10^{10}$          | $9,8 \cdot 10^9$          | $9,1 \cdot 10^9$          | $8,5 \cdot 10^9$          |
| $10^{-4}$ | $1.0 \cdot 10^9$             | $9,8 \cdot 10^8$          | $9,1 \cdot 10^8$          | $8,5 \cdot 10^8$          |
| $10^{-3}$ | $1.0 \cdot 10^8$             | $9,8 \cdot 10^7$          | $9,1 \cdot 10^7$          | $8,5 \cdot 10^7$          |
| $10^{-2}$ | $1.0 \cdot 10^7$             | $9,8 \cdot 10^6$          | $9,2 \cdot 10^6$          | $8,6 \cdot 10^6$          |
| 0, 1      | $1.0 \cdot 10^6$             | $1,0 \cdot 10^6$          | $9,6 \cdot 10^5$          | $9,0 \cdot 10^5$          |
| 2/3       | $2,7 \cdot 10^5$             | $2,5 \cdot 10^5$          | $2,4 \cdot 10^5$          | $2,2 \cdot 10^5$          |
| 0, 9      | $3,6 \cdot 10^5$             | $3,4 \cdot 10^5$          | $3,2 \cdot 10^5$          | $3,0 \cdot 10^5$          |
| 0, 99     | $1.0 \cdot 10^6$             | $9,9 \cdot 10^5$          | $9,2 \cdot 10^5$          | $8,6 \cdot 10^5$          |
| 0, 9999   | $1.0 \cdot 10^7$             | $9,8 \cdot 10^6$          | $9,1 \cdot 10^6$          | $8,5 \cdot 10^6$          |
| 0, 999999 | $1.0 \cdot 10^8$             | $9,8 \cdot 10^7$          | $9,1 \cdot 10^7$          | $8,5 \cdot 10^7$          |
| $C_{max}$ | $4.2 \cdot 10^8$             | $3,6 \cdot 10^8$          | $3,0 \cdot 10^8$          | $2,3 \cdot 10^8$          |

Table 9: Masses of gas clouds in the centre  
of axially symmetric anisotropies  
for  $b = 10$  ( $T_1 = 1,08 \cdot 10^3$  K,  $q = 0,0083$ )

| $C$         | $M/M_{\odot}(\alpha = 0, 5)$ | $M/M_{\odot}(\alpha = 1)$ | $M/M_{\odot}(\alpha = 2)$ | $M/M_{\odot}(\alpha = 5)$ |
|-------------|------------------------------|---------------------------|---------------------------|---------------------------|
| $C_{min}$   | $2,3 \cdot 10^{12}$          | $1,7 \cdot 10^{12}$       | $1,3 \cdot 10^{12}$       | $8,6 \cdot 10^{11}$       |
| $10^{-7}$   | $1.1 \cdot 10^{12}$          | $1,0 \cdot 10^{12}$       | $9,7 \cdot 10^{11}$       |                           |
| $10^{-6}$   | $1.1 \cdot 10^{11}$          | $1,0 \cdot 10^{11}$       | $9,7 \cdot 10^{10}$       | $9,4 \cdot 10^{10}$       |
| $10^{-5}$   | $1.1 \cdot 10^{10}$          | $1,0 \cdot 10^{10}$       | $9,7 \cdot 10^9$          | $9,4 \cdot 10^9$          |
| $10^{-4}$   | $1.1 \cdot 10^9$             | $1,0 \cdot 10^9$          | $9,7 \cdot 10^8$          | $9,4 \cdot 10^8$          |
| $10^{-3}$   | $1.1 \cdot 10^8$             | $1,0 \cdot 10^8$          | $9,7 \cdot 10^7$          | $9,4 \cdot 10^7$          |
| $10^{-2}$   | $1.1 \cdot 10^7$             | $1,0 \cdot 10^7$          | $9,8 \cdot 10^6$          | $9,5 \cdot 10^6$          |
| $0, 1$      | $1.1 \cdot 10^6$             | $1,1 \cdot 10^6$          | $1,0 \cdot 10^6$          | $9,9 \cdot 10^5$          |
| $2/3$       | $2,8 \cdot 10^5$             | $2,6 \cdot 10^5$          | $2,5 \cdot 10^5$          | $2,5 \cdot 10^5$          |
| $0, 9$      | $3,8 \cdot 10^5$             | $3,6 \cdot 10^5$          | $3,4 \cdot 10^5$          | $3,3 \cdot 10^5$          |
| $0, 99$     | $1.1 \cdot 10^6$             | $1,0 \cdot 10^6$          | $9,8 \cdot 10^5$          | $9,5 \cdot 10^5$          |
| $0, 9999$   | $1.1 \cdot 10^7$             | $1,0 \cdot 10^7$          | $9,7 \cdot 10^6$          | $8,5 \cdot 10^6$          |
| $0, 999999$ | $1.0 \cdot 10^8$             | $1,0 \cdot 10^8$          | $9,7 \cdot 10^7$          | $9,4 \cdot 10^6$          |
| $C_{max}$   | $7.0 \cdot 10^8$             | $5,9 \cdot 10^8$          | $5,1 \cdot 10^8$          | $4,0 \cdot 10^8$          |

Table 10: Masses of gas clouds in the centre  
of axially symmetric anisotropies  
for  $b = 20$  ( $T_1 = 0,792 \cdot 10^3$  K,  $q = 0,0024$ )

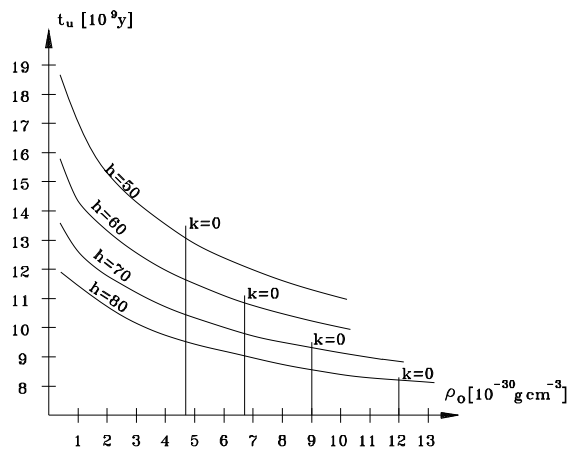


Fig.1: The age  $t_u$  of the universe depending  
on the Hubble-parameter  
 $H_0 = h \cdot \text{km/sec} \cdot \text{Mpc}$  and the  
present day density  $\rho_0$